Available online at www.sciencedirect.com
SCIENCE DIRECT®
Journal of Magnetic Resonance 177 (2005) 129–138
JMR Journal of Magnetic Resonance
www.elsevier.com/locate/jmr

Detection of intracellular lactate with localized diffusion {^{1}H–^{13}C}-spectroscopy in rat glioma in vivo

Josef Pfeuffer *, Joseph C. Lin, Lance DelaBarre, Kamil Ugurbil, Michael Garwood

Center for Magnetic Resonance Research, Department of Radiology, University of Minnesota Medical School, 2021 6th Street S.E., Minneapolis, MN 55455, USA

Received 15 March 2005; revised 13 July 2005
Available online 18 August 2005

Abstract

The aim of this study was to compare the diffusion characteristic of lactate and alanine in a brain tumor model to that of normal brain metabolites known to be mainly intracellular such as *N*-acetylaspartate or creatine. The diffusion of ^{13}C-labeled metabolites was measured in vivo with localized NMR spectroscopy at 9.4 T (400 MHz) using a previously described localization and editing pulse sequence known as ACED-STEAM ('adiabatic carbon editing and decoupling'). ^{13}C-labeled glucose was administered and the apparent diffusion coefficients of the glycolytic products, {^{1}H–^{13}C}-lactate and {^{1}H–^{13}C}-alanine, were determined in rat intracerebral 9L glioma. To obtain insights into {^{1}H–^{13}C}-lactate compartmentation (intra- versus extracellular), the pulse sequence used very large diffusion weighting (50 ms/μm^2). Multi-exponential diffusion attenuation of the lactate metabolite signals was observed. The persistence of a lactate signal at very large diffusion weighting provided *direct* experimental evidence of significant *intracellular* lactate concentration. To investigate the spatial distribution of lactate and other metabolites, ^{1}H spectroscopic images were also acquired. Lactate and choline-containing compounds were consistently elevated in tumor tissue, but not in necrotic regions and surrounding normal-appearing brain. Overall, these findings suggest that lactate is mainly associated with tumor tissue and that within the time-frame of these experiments at least some of the glycolytic product ([^{13}C] lactate) originates from an intracellular compartment.

Keywords: Intracellular lactate; Distribution space; Cerebral metabolites; Rat brain in vivo; Glioma; Diffusion-weighted {^{1}H–^{13}C} NMR spectroscopy

1. Introduction

Diffusion NMR spectroscopy of cerebral metabolites is difficult to perform in vivo due to the limited spectral separation and signal-to-noise ratio. Diffusion coefficients are determined from the metabolite signal measured as a function of increasing diffusion weighting, which attenuates the already weak signal of metabolites (at concentrations in the order of 1–10 mM). Therefore, previous in vivo diffusion NMR spectroscopy experiments have been performed mainly with protons, although a couple of studies used other nuclei such as ^{31}P and ^{19}F, see [1,2] and references therein. Substantial improvements in sensitivity and spectral resolution in localized ^{1}H NMR spectroscopy have been demonstrated recently using high magnetic fields [3,4], by which the number of detectable metabolites and the range of measurable diffusion coefficients were expanded significantly [5,6].

The signals from cerebral metabolites measured with large diffusion weighting were shown to provide valuable information about their distribution between the intra- and extracellular space of the rat brain in vivo [6].

* Corresponding author. Present address: Siemens Medical Solutions, MREA-Neuro, Karl-Schall-Strasse 6, 91052 Erlangen, Germany. Fax: +49 9131 84 3083.
E-mail address: josef.pfeuffer@siemens.com (J. Pfeuffer).

1090-7807/$ - see front matter © 2005 Elsevier Inc. All rights reserved.
doi:10.1016/j.jmr.2005.07.010

With diffusion NMR spectroscopy, the intracellular signal has been previously separated from the extracellular signal at large diffusion weighting (large b values), because the apparent diffusion coefficient (ADC[1] D^{app}) in the intracellular compartment is one order of magnitude lower at large diffusion weighting [7]. Water and metabolites experience restrictions in their self-diffusion by membranes [8], as demonstrated by NMR measurements at large diffusion weighting in immobilized cells and the rat brain [9–11]. Thus, intracellular molecules show a *restricted diffusion* characteristic, where the mean displacement of molecules is constrained and limited at sufficiently large diffusion times [1,2]. The signal from an intracellular metabolite such as *N*-acetylaspartate (NAA) was shown to be non-monoexponential [10]. In another type of experiment using a glial tumor cell line, the extracellular water signal contribution was eliminated by a contrast agent and residual water signal from the intracellular space exhibited multiple components with diffusion coefficients being one to two orders of magnitude lower than free and hindered diffusion [12]. In general, the intracellular diffusion attenuation in vivo is influenced by shape and size of cells and their heterogenic distributions in the tissue, which in vivo is observed as a non-monoexponential attenuation. Often a *multi*-exponential analysis containing two to four components has been used to describe the measured signal decay empirically; a Laplace analysis, however, has shown that a distribution of components more accurately describes the non-monoexponential attenuation in the rat brain in vivo [5] as it is expected from theoretical modeling and evidence from porous media, see, for example [9,13].

In the extracellular space of in vivo brain, a *hindered diffusion* characteristic is observed, in which molecules have to move around obstacles and the diffusion path length is prolonged compared to free diffusion [14]. The apparent diffusion coefficient is thereby decreased by the so-called tortuosity factor. To a first approximation, the decay of signal from the extracellular space can be modeled to be mono-exponential with a reduced D^{app}; random-walk simulations in a spherical cell model, however, indicated that a deviation from a strictly mono-exponential decay can be observed at large diffusion weighting [15].

Only few studies of diffusion ^{13}C spectroscopy were reported in vitro [16–18]. The long acquisition times and techniques used in these previous studies were not targeted for in vivo application, and thus were not optimal for our studies. In this work, indirect ^{1}H detection of ^{13}C label with the 'adiabatic carbon editing and decoupling' (ACED) sequence [9,19] was used to measure, for the first time, signals of ^{13}C-labeled lactate (Lac) in vivo at very large diffusion weighting. In general, indirect detection of ^{13}C label via ^{1}H, denoted by $\{^{1}H–^{13}C\}$, is more sensitive compared with direct ^{13}C detection due to the higher gyromagnetic ratio of ^{1}H compared to ^{13}C. ^{13}C-labeling provides more *specific* information, since the natural abundance ^{13}C signal is low and thus the measured ^{13}C label originates mainly from the metabolism of the infused exogenous substrate. The infusate, e.g., ^{13}C-labeled glucose (Glc), is detected together with its metabolic products. In healthy brain metabolism, label of [^{13}C] Glc is incorporated into glutamate (Glu) and glutamine (Gln) via the TCA cycle; in a tumor, non-oxidative glucose consumption leads to ^{13}C-labeled Lac and alanine (Ala) [20–26].

In addition to their metabolic specificity, ^{13}C methods are advantageous because *unwanted* proton signals (e.g., from compounds lacking the ^{13}C label) can be eliminated. In studies of tumors that typically have intense mobile lipid signals such as breast cancer, the latter advantage is particularly important since intense resonances from mobile lipids overlap the Lac resonance at 1.32 ppm, which is the most intense Lac resonance because it arises from the three magnetically equivalent protons of the methyl group. The above mentioned metabolic specificity with the ^{13}C label also provides a spatial selectivity and localizes the measured signal directly in the metabolically active site in the tissue of interest. ACED-STEAM acquires ^{1}H spectral information simultaneously with ^{13}C signals. This is important because in the tumor ^{1}H signals from other metabolites of interest, like choline (Cho), Glu, glycine (Gly), taurine (Tau), and phosphorylethanolamine (PE), are measurable. The concentration of Lac, an end-product of non-oxidative glucose metabolism, is often elevated in neoplasms. Likewise, other important ^{1}H metabolites, such as Cho and mobile lipids, are elevated in malignant tumors.

Diffusion experiments with ^{13}C-labeled Lac are expected to provide further information regarding the compartmentation of the metabolically active Lac in a rat brain tumor model in vivo. Complementary information was acquired using ^{1}H spectroscopic imaging (CSI) of Lac and Cho in the tumor to assess the spatial distribution in primary tumor tissue, surrounding, and necrotic areas. Since the voxel used for diffusion $\{^{1}H–^{13}C\}$ spectroscopy contained inhomogeneous tissue contribution, ^{1}H CSI of pure Lac and Cho could help to clarify the location and spatial distribution of the metabolite signals in the $\{^{1}H–^{13}C\}$ data. An objective of this study was to compare the multi-exponential diffusion characteristic of Lac *in a tumor* to that of metabolites known to be mainly intracellular like NAA, creatine (Cr + PCr), glutamate, *myo*-inositol (Ins), or Tau. The detection of a Lac signal at very large diffusion weighting could provide *direct* experimental evidence of *intracellular* Lac in a tumor.

[1] *Abbreviations used:* NAA, *N*-acetylaspartate; Ala, alanine; ADC, apparent diffusion coefficient; Cho, choline-containing compounds; Cr, creatine; Glc, glucose; Gln, glutamine; Glu, glutamate; Gly, glycine; Ins, *myo*-inositol; Lac, lactate; MM, macromolecule; PCr, phosphocreatine; PE, phosphorylethanolamine; Tau, taurine.

Preliminary results of this work have been published in abstract form [27,28].

2. Methods

2.1. Animal preparation

Eight male Fisher rats (300–400 g, 5 in the 4.7 T and 3 in the 9.4 T studies) were measured 12–14 days after inoculation with 9L glioma into the right hemisphere, 3 mm from the midline and 1 mm posterior to the bregma (10 μL of cell suspension at 1×10^5 cells/μL). Voxels of 60–180 μL volume were chosen to include most of the tumor tissue. For the MR experiment, the rats were anesthetized with 2% isoflurane in 60%/40% O_2/N_2O, and ventilated at physiological conditions. Oxygen saturation, maintained above 95%, was continuously monitored with an infrared sensor clipped to the tail (Nonin Medical, Minneapolis, MN). A rectal thermosensor (Cole-Parmer, Vernon Hills, IL) was used to verify that the body temperature was at 37 °C, which was maintained by placing the rats on a heated water blanket. A femoral venous line was used for infusion of 100% enriched [1-^{13}C] D-glucose (Isotec, Miamisburg, OH). In all studies, a bolus of 200 mg Glc was given in the first 5 min, followed by a constant-rate Glc infusion of 16 mg/min, which typically led to modestly elevated plasma Glc concentrations on the order of 16 mM, similar to previous animal studies [9,19]. A steady state of [1-^{13}C] D-Glc turnover into [3-^{13}C] Lac was achieved in the tumor voxel after approximately 1 h of continuous i.v. infusion.

2.2. MR hardware

{^{1}H–^{13}C} NMR spectroscopy was performed with a Varian INOVA spectrometer (Varian, Palo Alto, CA) interfaced to a 31-cm horizontal bore, 9.4 T magnet (Magnex Scientific, Abingdon, UK). The 11-cm actively shielded gradient insert was capable of switching 300 mT/m in 500 μs in each direction (Magnex Scientific, Abingdon, UK). More details of hardware and methods used for indirect ^{13}C detection were described previously [6,19]. A quadrature 400 MHz ^{1}H surface RF coil, combined with a linearly polarized, three-turn 100 MHz ^{13}C coil with a diameter of 12 mm, was used for transmission and reception [19].

^{1}H CSI experiments were performed on an Oxford 4.7 T/40-cm bore magnet interfaced to a Varian INOVA spectrometer. A 15-mm diameter surface coil was used for RF transmission and detection at 200 MHz.

2.3. ^{1}H MR spectroscopy

The localization for in vivo MR spectroscopy was based on a short echo time STEAM sequence combined with VAPOR water suppression and interleaved outer volume suppression [29]. Shimming of all first- and second-order shim coils was done with FASTMAP [30], typically resulting in 18–26 Hz linewidth (0.045–0.065 ppm) of the water resonance in voxels with 60–180 μL volume covering most of the tumor.

2.4. ^{13}C editing

The localizing ACED-STEAM sequence is illustrated in Fig. 1. For ^{13}C editing, a 15-ms long adiabatic full passage (AFP) pulse of the HS8 type [31] with a 12 kHz bandwidth for 99% inversion efficiency was applied during the middle period TM on the ^{13}C channel. Broadband adiabatic decoupling [19] or WALTZ-16 decoupling with 1 kHz width (10 ppm) was applied in the carbon channel during the entire acquisition. Switching the carbon editing pulse on and off alternately resulted in two ^{1}H spectra that were recorded separately, denoted ACED^{ON} and ACED^{OFF}. Inherently, the ACED^{OFF} spectrum, obtained in the absence of the editing pulse, contains the total ^{1}H signals bound to ^{12}C and ^{13}C, which is expressed by the nomenclature {^{1}H-[^{12}C + ^{13}C]}. The ACED^{ON} spectrum, obtained in the presence of the editing pulse, contains the ^{1}H signals bound to ^{12}C and the *inverted* ^{1}H signals bound to ^{13}C, indicated by {^{1}H-[^{12}C–^{13}C]}. Subtraction of the spectrum ACED^{ON} from ACED^{OFF} filters the signal from protons bound to ^{13}C only, thus resulting in the edited {^{1}H–^{13}C} signals. The theoretical signal dependence with respect to J_{CH} coupling is proportional to $\cos(\pi TE \cdot J_{CH})$. Our minimum TE was determined by the duration of the diffusion gradients and chosen to be $TE = 3/J_{CH}$ with the couplings constant $J_{CH} \sim 127$ Hz for Lac.

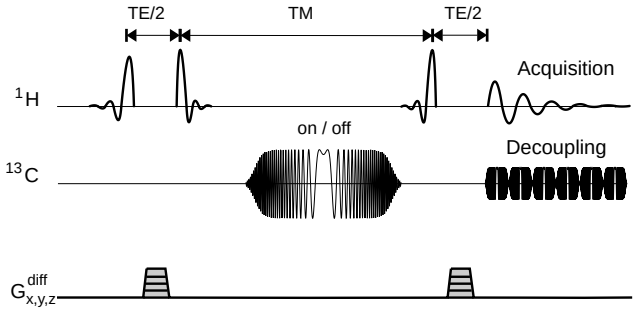

Fig. 1. Adiabatic carbon editing and decoupling (ACED) sequence with diffusion gradients. Single voxel localization and signal acquisition is done with a STEAM scheme (^{1}H); the localizing gradients are omitted here for better clarity. On the ^{13}C channel, an adiabatic inversion pulse is applied in interleaved scans during the middle period TM. ^{13}C decoupling was applied during acquisition. The echo time TE was set to $3/J_{CH}$ (23 ms, optimized for lactate). For diffusion weighting, gradients in x, y, z-direction were applied during the first and second TE/2 period with constant duration of 8 ms, separation 122 ms, and varying amplitude.

2.5. Diffusion weighting

In addition to ACED-STEAM, unipolar gradients for diffusion weighting of the ^{1}H–^{13}C NMR signals of metabolites were placed during the TE/2 periods in the STEAM sequence [5,6]. The strength of the diffusion attenuation was characterized by the parameter $b = (\gamma^2 \cdot G^2 \cdot \delta^2) \cdot t_D$, where G is the gradient strength, δ is the duration of the gradient pulses, and $t_D = \Delta - \delta/3$ is the diffusion time, where Δ is the time separating gradient pulses. Diffusion coefficients [D] are expressed in units of $\mu m^2/ms$ ($= 10^{-9}$ m^2/s) and the b values [b] have units of $ms/\mu m^2$ ($= 10^9$ s/m^2). Experiments were performed with constant diffusion time t_D, whereby the gradient strength was varied. In the first type of experiments, a b range from 0 to 5 $ms/\mu m^2$ was covered, linearly increasing G (eight points). In the second type of experiments, four b values were chosen, at $b = 0$ as a reference and at 15, 30, and 50 $ms/\mu m^2$. In both types of experiments, the signals at different b values were recorded in an interleaved manner, with $\delta = 8$ ms, $\Delta = 122.3$ ms, and $t_D = 119$ ms. Gradients were applied in all three directions simultaneously.

2.6. Processing

Data analysis, modeling, and fitting were performed similarly as described recently [6]. The FID data from each scan were stored separately. The sensitivity was sufficient to permit automated correction of the phase and frequency of single-scan metabolite spectra at all b values despite a fully suppressed water signal. The apparent diffusion coefficients (ADC, D^{app}) of the metabolites were determined from the negative slope of the signal attenuation versus b value, i.e., $\ln S/S_0 = -b \cdot D^{app}$. Log-linear regression was used to fit the data in the b range of 0–5 $ms/\mu m^2$. The apparent diffusion coefficient was termed ADC at small b values as it is common in the literature. The data of the full b range of 0–50 $ms/\mu m^2$ were analyzed by bi-exponential fitting according $S/S_0 = p_1^{app} \exp(-b \cdot D_1^{app}) + p_2^{app} \exp(-b \cdot D_2^{app})$, constraining the sum of the volume fractions to one ($p_1^{app} + p_2^{app} = 1$). The population fractions p_1^{app} and p_2^{app} are 'apparent,' because they are not straightforward to interpret and do not directly correspond to extracellular and intracellular compartment fractions (see Section 3).

2.7. ^1H chemical shift imaging

Two-dimensional spectroscopic imaging of Lac, Cho, and lipids in intracerebral 9L gliomas was done with a water-suppressed, homonuclear-edited ^{1}H CSI sequence at 4.7 T ($N = 5$). With a double spin-echo pulse sequence, as described previously [28], Lac editing and water suppression were performed simultaneously by a pair of asymmetric frequency-selective pulses capable of producing an extremely sharp transition band on one side of the inverted region. The asymmetric AFP pulse was generated by splicing two different adiabatic passage pulses together as described previously [32]. Separation of Lac from other metabolites was based on J-difference editing, which required a minimum of two excitations. Lac was edited by subtracting alternate FIDs, whereas a normal ^{1}H metabolite spectrum minus the Lac resonance was obtained by adding alternate FIDs.

Metabolite maps of the CSI data were generated using the Varian CSI data processing tool. The raw CSI data with a nomial voxel size of $1.6 \times 1.6 \times 2$ mm^3 (16×16 matrix) were processed through spatial and spectral reconstruction. In the spatial domain, a DC correction and a Gaussian filter was applied; in the spectral domain, phase and baseline correction, and linebroadening with 10 Hz were performed globally. After peak picking and curve fitting with Gaussian/Lorentzian lines, the metabolite spatial information was taken from the integral. For final display, the 16×16 metabolite maps were spatially smoothed by interpolation to 256×256. To produce the anatomical outline background for the metabolite maps, the spin-echo image was blurred and filtered with an edge detection kernel. The metabolite map was then superimposed over the anatomical outline.

3. Results and discussion

3.1. Phantom experiments

Experimental performance of the diffusion-weighted {^{1}H–^{13}C} ACED-STEAM sequence was tested and calibrated in phantoms using a 20 mM [3-^{13}C] Lac solution (60% enriched). Two series of spectra are shown in Figs. 2A and B with the ^{13}C editing pulse switched on ($ACED^{ON}$) and off ($ACED^{OFF}$), respectively, with ^{13}C-decoupling turned off in both experiments. Subtraction of these alternately recorded spectra yielded the doublet of ^{13}C-labeled Lac. With ^{13}C-decoupling switched on (Figs. 2C and D), single resonance proton spectra of Lac (doublet at 1.32 ppm) were obtained representing either total (^{12}C + ^{13}C-labeled) Lac (Fig. 2C) or solely ^{13}C-labeled Lac (Fig. 2D). With diffusion weighting up to 1.9 $ms/\mu m^2$, strictly mono-exponential attenuation curves were found for {^{1}H–^{12}C} and {^{1}H–^{13}C} signals (Fig. 2). The diffusion coefficient was (1.20 ± 0.06) $\mu m^2/ms$ at 23 °C and was attributed to free diffusion of Lac in water solution [6,33]. For in vivo conditions at 37 °C, the free diffusion coefficient for Lac is expected to be further increased.

3.2. Localized NMR spectroscopy in 9L glioma

Single voxel spectroscopy of intracerebral tumor (9L glioma) was performed with the diffusion-weighted

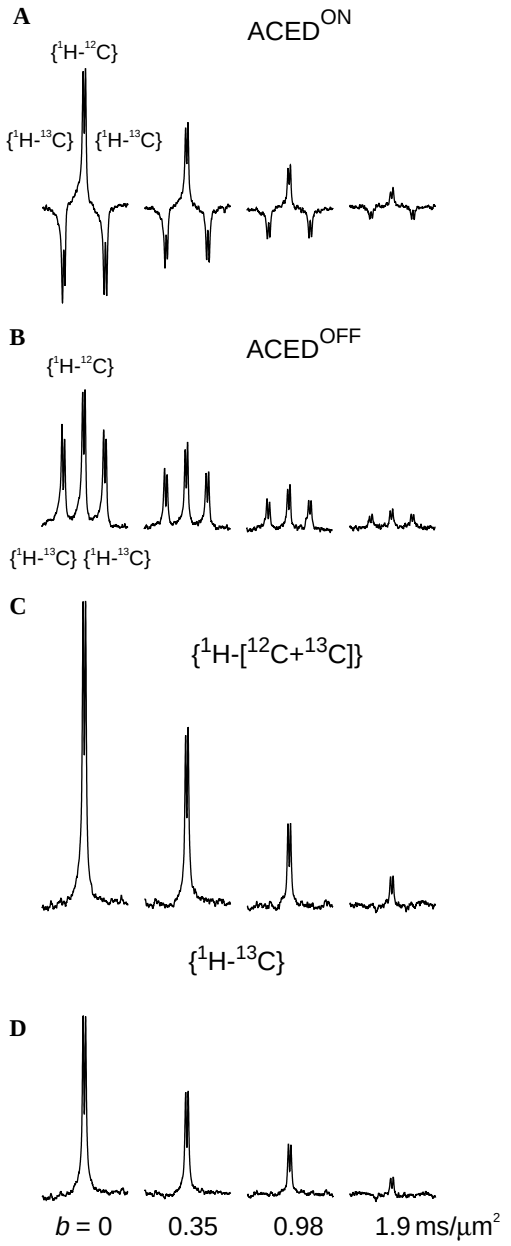

Fig. 2. ACED-STEAM spectra of Lac at 1.32 ppm ([3-^{13}C]-labeled, 60% enriched, 20 mM) with increasing diffusion weighting up to 1.9 ms/μm^2. (A and B) The {^{1}H–^{13}C} signals of Lac were inverted (ACED^{ON}) when ^{13}C inversion pulse was switched on (A) and non-inverted (ACED^{OFF}), when the ^{13}C inversion pulse was off (B). Decoupling during acquisition was switched off in (A and B) for demonstration of the method to separate {^{1}H–^{12}C} and {^{1}H–^{13}C} signals at 1.32 and 1.26/1.37 ppm, respectively. (C and D) With decoupling, {^{1}H–^{12}C} and {^{1}H–^{13}C} signals of Lac are superimposed at 1.32 ppm. Subtraction of ACED^{OFF} and ACED^{ON} spectra yields the ^{13}C-filtered signal {^{1}H–^{13}C} (D). The additional applied diffusion gradients encode a strictly mono-exponential signal decay due to free diffusion of Lac in water solution (23 °C). Acquisition parameters: single-voxel spectroscopy using ACED-STEAM with VAPOR water suppression, voxel size $7 \times 3 \times 7$ mm^3, NA 8, SW 5 kHz, TE 23.4 ms, TM 20 ms, TR 4 s. Diffusion-weighted ACED with AFP inversion (HS8 type, 15 ms duration), adiabatic decoupling with HS8-pattern, diffusion parameters $\delta = 5$ ms and $\Delta = 122.3$ ms, Gaussian windowing $gf = 0.2$ s.

ACED-STEAM sequence in the rat brain at 9.4 T. Anatomical spin-echo images in transverse and coronal orientation are shown in Figs. 3A and B with the voxel indicated. The dark region in the center of the tumor was attributed to necrosis. The outer boundaries of the tumor tissue were also discernible in contrast to the surrounding healthy tissue. The CSF of ventricles was visible as bright signal in the MR images. On the right hemisphere of the brain, the mass effect from the growing tumor compressed the ventricle and corresponding tissue to the posterior regions. Fig. 3C shows the localized ^{1}H spectrum of metabolites from the 132-μL voxel in the tumor. The spectral linewidth measured from the ^{1}H water signal in the voxel was 0.065 ppm (26 Hz). The neurochemical profile was different from ^{1}H spectra in the healthy rat brain. NAA and Cr + PCr levels in the tumor were decreased considerably in comparison with normal brain. In contrast, contributions of Lac (1.32 ppm), Ala (1.47 ppm), Cho (3.21 ppm), and Gly (3.56 ppm) were clearly detectable and elevated in the tumor. Further detected metabolites were Glu (2.35 and 3.75 ppm), Tau (3.42 ppm), and PE (3.98 ppm). Also, contributions from macromolecules—visible at the short echo time of 23 ms—could be assigned at 0.9 and 2.0 ppm based on peak positions and their broad linewidths.

3.3. Diffusion {^{1}H–^{13}C} spectroscopy

Lac (1.32 ppm) and Ala (1.47 ppm) peaks obtained with diffusion-weighted ^{13}C ACED-STEAM spectra in the rat glioma in vivo are shown in Fig. 4. Pairs of ^{13}C-inverted and non-inverted ^{1}H spectra are plotted in Fig. 4A as indicated by the brackets. Similar to the phantom data in Fig. 2, the ^{13}C inversion pulse was switched on (ACED^{ON}) and off (ACED^{OFF}), and the data were acquired in an interleaved manner. As indicated by the dotted lines, the indirectly detected ^{13}C signal {^{1}H–^{13}C} arose from the difference of the non-inverted {^{1}H-[^{12}C + ^{13}C]} and the ^{13}C-inverted {^{1}H-[^{12}C–^{13}C]} spectra. In Fig. 4B, the difference {^{1}H–^{13}C} signals are shown with an amplification factor of four, in which only protons bound to ^{13}C were observed (edited for $J_{CH} = 127$ Hz). The ACED-STEAM spectra of Lac and Ala were measured with a diffusion weighting from $b = 0$ to 4.9 ms/μm^2. Diffusion time was constant at 119 ms. The apparent diffusion coefficient (ADC) was calculated from the mono-exponential signal decay of Ala and Lac resonances at these relatively low b values. The results from three studies are summarized in Table 1; in study #1, the Ala signal was not detectable. The ADC values were (0.13 ± 0.02) μm^2/ms for {^{1}H–^{13}C}-Lac ($N = 3$, mean ± std) and (0.16 ± 0.02) μm^2/ms for {^{1}H–^{13}C}-Ala ($N = 2$).

In the second part of the sessions, ACED-STEAM spectra of 9L glioma were additionally measured at very large diffusion-weighting from $b = 15$ to 50 ms/μm^2. The

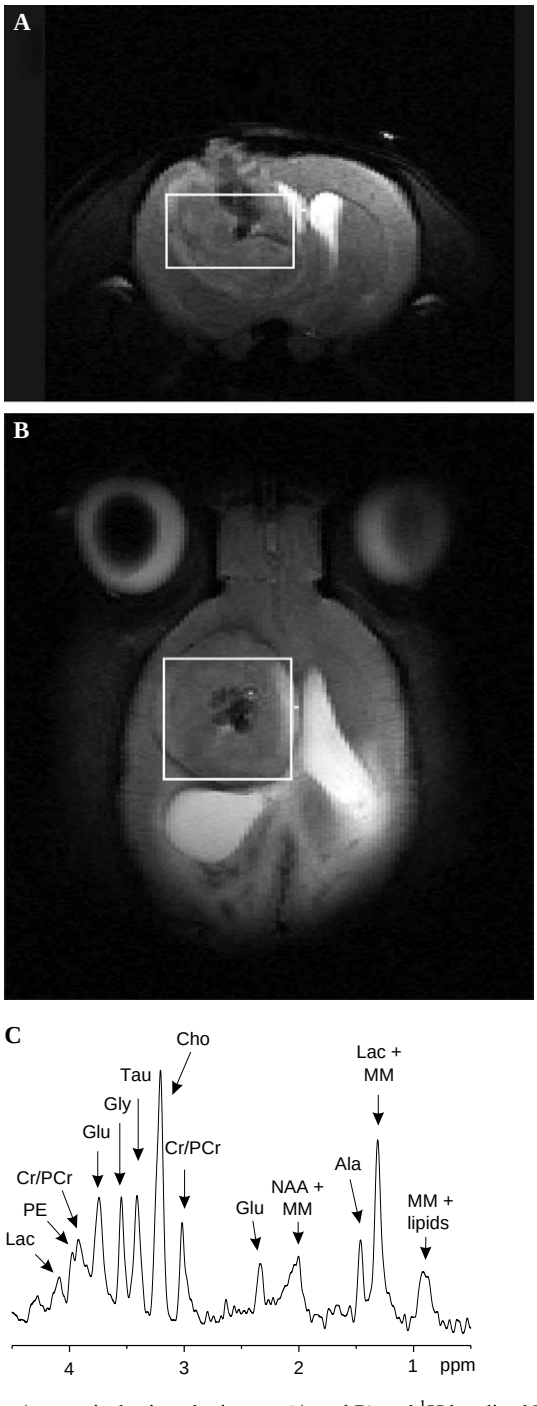

Fig. 3. Anatomical spin-echo images (A and B) and ^{1}H localized NMR spectrum (C) of 9L glioma in the rat brain at 9.4 T. The voxel for diffusion-weighted ACED spectroscopy is shown in coronal (A) and axial view (B) covering most of the tumor. The dark region in the center of the tumor indicates a necrotic area. The outer boundaries of tumor tissue are also discernible. The CSF of ventricles is visible as bright signal in the MR images. (C) The localized ^{1}H metabolite spectrum of the tumor is considerably different from healthy brain: NAA and Cr + PCr content is significantly decreased; in contrast, Lac, Ala, Cho, and Gly contributions are increased. Acquisition parameters: Adiabatic spin-echo sequence, field of view 3×3 cm^2, matrix 256×128, 2 mm slice thickness, nominal resolution $0.12 \times 0.23 \times 2$ mm^3, SW 27 kHz, TE 60 ms, TR 0.8 s. Single-voxel ^{1}H spectroscopy with STEAM localization and VAPOR water suppression, voxel size $6.6 \times 4 \times 5$ mm^3, NA 240, SW 5 kHz, TE 23 ms, TR 4 s.

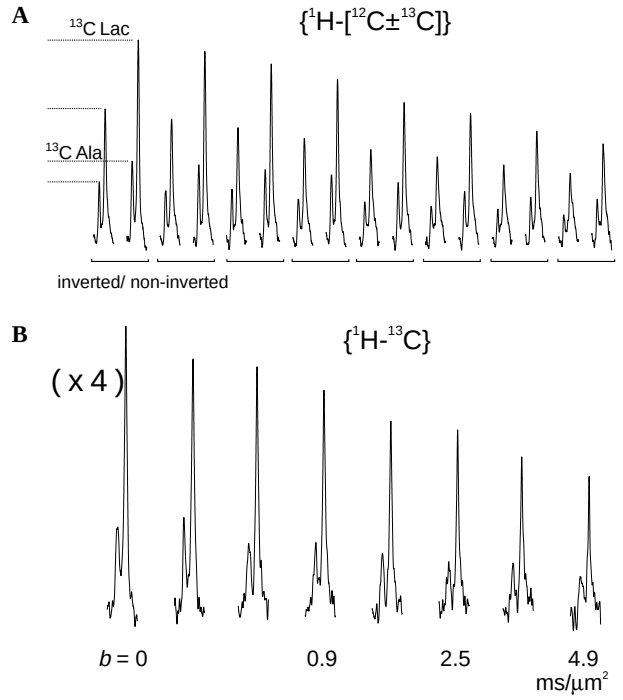

Fig. 4. Diffusion-weighted ACED spectra (^{13}C-edited Lac and Ala) of 9L glioma in the rat brain in vivo at 9.4 T. (A) Pairs of ^{13}C-inverted {^{1}H-[^{12}C–^{13}C]} and non-inverted {^{1}H-[^{12}C + ^{13}C]} ^{1}H spectra of Lac (1.32 ppm) and Ala (1.47 ppm) are shown, in which the ^{13}C inversion pulse was switched on and off, respectively. As indicated by the dotted lines, the edited {^{1}H–^{13}C} signal arises from the difference of the non-inverted and ^{13}C-inverted spectra. (B) Edited {^{1}H–^{13}C} signals of Lac and Ala with moderate diffusion weighting from 0 to 4.9 ms/μm^2. Acquisition parameters: diffusion-weighted ACED-STEAM with VAPOR water suppression, voxel size $6.6 \times 4 \times 5$ mm^3, NA 240, SW 5 kHz, TE 23 ms, TR 4 s. Diffusion-weighted ACED with AFP inversion (HS8 type, 15 ms duration), WALTZ decoupling, diffusion parameters $\delta = 8$ ms and $\Delta = 122$ ms.

Table 1
Apparent diffusion coefficients of {^{1}H–^{13}C}-alanine and {^{1}H–^{13}C}-lactate in rat 9L glioma in vivo derived from the signal attenuation at small b values

Study	ADC (Ala)[a] (μm^2/ms)	ADC (Lac) (μm^2/ms)
#1	—[b]	0.11 ± 0.01
#2	0.16 ± 0.02	0.14 ± 0.01
#3	0.16 ± 0.02	0.15 ± 0.01
Mean ± std[c]	0.16 ± 0.02	0.13 ± 0.02

[a] Apparent diffusion coefficients were fitted from mono-exponential signal decay in the range of $b = 0$–5 ms/μm^2 for Ala and Lac resonances, respectively.
[b] No Ala signal was detectable in study #1.
[c] For calculation of the standard deviation (std), the square root of the sum of the squares of the individual errors was taken.

diffusion-attenuated signal of {^{1}H–^{13}C}-Lac revealed a fast and a slow decaying diffusion components (Fig. 5). The signal-to-noise ratio of the {^{1}H–^{13}C}-edited spectra of Lac was still reasonable given the low abundance and sensitivity of ^{13}C; signals were well detectable

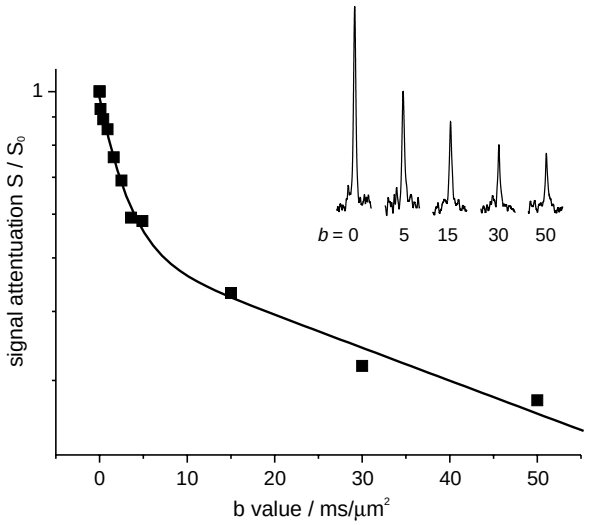

Fig. 5. ACED spectra (^{13}C-edited Lac) of 9L glioma at large diffusion-weighting. The diffusion attenuated signal of {^{1}H–^{13}C} Lac revealed a fast and a slow diffusion component, which were fit by a bi-exponential decay curve (solid line). The {^{1}H–^{13}C}-edited spectra of Lac show a very good signal-to-noise ratio and are well detectable even at large diffusion weighting of 50 ms/μm^2 (see inset). Acquisition parameters: diffusion-weighted ACED-STEAM with VAPOR water suppression similar as in Fig. 4, voxel size $4.1 \times 3 \times 4.7$ mm^3, NA 160 (at low b) and 224 (at large b).

even at very large diffusion weighting (see Fig. 5, inset). A nonlinear fit to a bi-exponential decay curve (Fig. 5, solid line) revealed the apparent diffusion coefficients $D_1^{app} = (0.36 \pm 0.06)$ μm^2/ms and $D_2^{app} = (0.014 \pm 0.003)$ μm^2/ms, respectively (see also Table 2). The fast and slow apparent diffusion coefficients differed by more than an order of magnitude. The apparent volume fraction p_2 of the slow component was (52 ± 4)%. A similar bi-exponential decay was found in a second study with $D_{1,2}^{app}$ of 0.20 and 0.005 μm^2/ms, respectively (see Table 2). The corresponding apparent volume fraction p_2 of 18% was significantly lower compared to study #1; the {^{1}H–^{13}C}-edited spectra of Lac were more attenuated at large diffusion weighting. In study #3, {^{1}H–^{13}C}-Lac signal was not detectable at large b values and thus could not be used for multi-exponential analysis.

Table 2
Apparent diffusion coefficients (D^{app}) and volume fractions (p^{app}) of {^{1}H–^{13}C}-lactate in rat 9L glioma in vivo derived from the signal attenuation at large b values

Study	D_1^{app} [a] (μm^2/ms)	D_2^{app} (μm^2/ms)	p_2^{app} (%)
#1	0.36 ± 0.06	0.014 ± 0.003	52 ± 4
#2[b]	0.20 ± 0.04	0.005 ± 0.01	18 ± 9

[a] $D_{1,2}^{app}$ and p_2^{app} were fitted from a bi-exponential decay in the range of $b = 0$–50 ms/μm^2 for Lac ($p_1^{app} + p_2^{app} = 1$). In all studies, Ala signal was not detectable at large b values. In study #3 (see Table 1), Lac signal was not detectable at large b values.

[b] Tumor size was more progressed and a factor of three larger compared to study #1.

{^{1}H–^{13}C}-Ala signals were not detected in any of the studies at large b values.

The feasibility of diffusion {^{1}H–^{13}C} spectroscopy was shown here as a new technique in vivo. Specifically, the diffusion characteristic of [3-^{13}C] Lac and [3-^{13}C] Ala in rat glioma could be measured during infusion of [1-^{13}C] Glc. ADC values of Lac and Ala (0.13 and 0.16 μm^2/ms) as evaluated in Table 1 were comparable to that of intracellular metabolites in normal rat brain (0.09–0.14 μm^2/ms) [6]. This data summarized in Table 1 already indicates that a significant portion of the metabolized ^{13}C label can be attributed to the intracellular compartment within the tumor tissue. If Lac would be in CSF, extracellular space, or the necrotic core, its ADC would be more similar to free diffusion and would be significantly increased to values in the range of 0.3–1.0 μm^2/ms. In addition, no or only little signal would be found at large b values.

The ADC of Lac reported here (0.13 μm^2/ms) is similar to a previous lactate diffusion measurements in tumors using a double-quantum coherence-transfer (DQCT) technique on a H-MESO-1 line [34–36], which reported values of (0.23 ± 0.02) and (0.21 ± 0.03) μm^2/ms. Since the diffusion time was considerably shorter (17.7 ms) [34] than that used in the current study (119 ms), the ADC of Lac is expected to be increased compared to our study due to the reduced exposure to restricting boundaries at shorter diffusion times. It cannot be excluded that also anisotropic effects could be found in these types of experiments, which would be possibly reflected in different ADC values of Ala and Lac in different directions. In our study, we used only a single diagonal direction.

Considering that we were not able to detect an Ala signal at large b values in any of the studies, one could model different compartmentation of Ala compared to Lac giving rise to different contributions to the ADC values. In this case, the diffusion characteristics could be different for tumor Lac versus tumor Ala and in comparison to metabolites measured in the healthy rat brain. We, however, attribute the absence of Ala signal at large b values at first hand to technical issues as opposed to potential physiological and biophysical interpretations of different compartmentation. As can be seen in Fig. 4B, the limits of signal-to-noise were nearly reached for Ala at a b value of 5 ms/μm^2. In this way, a comparison of Lac and Ala diffusion might be valid only for the ADC at smaller b values.

The clearly detectable {^{1}H–^{13}C}-Lac signal at b values of 50 ms/μm^2 (shown in Fig. 5 and Table 2) is direct evidence that some detectable fraction of Lac undergoes highly restricted diffusion and thus is localized inside the cells. In a previous study of healthy rat brain, the bi-exponential diffusion characteristic and apparent volume fractions p_2^{app} of cerebral metabolites were very similar for intracellular metabolites, such as NAA and Cr,

and the values of these parameters differed from those of metabolites known to have extracellular fractions, such as Glc and Lac [6]. Our diffusion data of study #1 measured in 9L glioma (see Table 1) show that the fitted parameters D_2^{app} and p_2^{app} are very similar to that of intracellular metabolites. In study #2, the signals at large b values were relatively low and p_2^{app} was correspondingly lower, which indicated that this tumor could have a smaller fraction of intracellular Lac. On the other hand, a reduced lactate signal at large b values could also be caused by increased intra/extracellular exchange and corresponding signal attenuation. The differences between the two studies #1 and #2 may be explained by differences in heterogeneity and histologic features in the tumors; the tumor in study #2 appeared to have progressed to a more advanced stage and was threefold larger than the tumor in study #1. Information about the lactate pool sizes (intra- versus extracellular) in tumors has implications for determining metabolic rates and lactate transport kinetics from modeling ^{13}C NMR data [25,37–40].

Due to the complexity of the in vivo situation, and considering the limited SNR and number of data points, we have analyzed the experimental diffusion attenuation by bi-exponential fitting, being aware of the limitations of this simplified analysis. Our reference was a previous study with similar setup and diffusion weighting of ^1H metabolite signal [6], which was performed in the healthy rat brain to separate intra- and extracellular diffusion components using the measured characteristics of NAA metabolite diffusion in the intracellular space as a reference. Based on this study, the signals at lower diffusion weighting (p_1^{app}) are expected to contain contributions from *both* extra- and intracellular signal, whereas a detectable signal at large diffusion weighting (p_2^{app}) can be taken as evidence for a predominately intracellular signal. Caution has to be taken, however, when interpreting the volume fraction of the component at large diffusion weighting (p_2^{app}) in terms of 'absolute' fraction of intracellular versus extracellular signal, since it contains only a part of the intracellular signal [6].

3.4. ^1H chemical shift imaging of 9L glioma

To image the spatial distribution of Lac in the tumor, a homonuclear-edited ^1H CSI sequence [28] was used for spectroscopic imaging. The chemical shift image of Lac in intracerebral 9L glioma is shown in Fig. 6B (red) superimposed on a T_2-weighted spin echo image (Fig. 6A). In all cases, Lac was detected in the tumor region only, which is consistent with previous findings [41]. Cho was also elevated in and around the tumor (Fig. 6C), whereas Cr and NAA levels were generally below detection in the tumors, similar to Fig. 3C. A common finding was that both Lac and Cho were non-uniformly distributed in the tumors. Lac was generally found in tumor areas that also exhibited high Cho levels (see Fig. 6, Lac and Cho CSI map). Specifically, in the necrotic areas in the center of the glioma, no Lac was found. This observation is consistent with the complementary $\{^1H–^{13}C\}$ metabolite diffusion data, which indicate that Lac is predominantly found intracellularily in the tumor tissue only. With this homonuclear editing method [28], Lac was edited and separated from overlapping resonances, which allowed the simultaneous detection of other ^1H metabolites, including mobile lipids (Fig. 6D). A further advantage was the built-in water suppression, i.e., additional RF pulses were not required to suppress water signal.

3.5. Features of diffusion $\{^1H–^{13}C\}$ spectroscopy

^{13}C-labeling captures specific information about tissue metabolism and distinguishes oxidative from non-oxidative glucose consumption based on the metabolic products. In several respects, the use of [1-^{13}C] Glc infusion is advantageous for the detection of Lac in a tumor model. Only signal from metabolically active tissue (Glc converted to Lac and Ala) is observed giving an intrinsic selectivity and localization in the tumor. The ^{13}C-editing technique eliminates unwanted lipid signals often found concomitant with the Lac signal in ^1H NMR spectra of tumors. The high concentration and ^{13}C-fractional enrichment of Lac in vivo is advantageous for spectroscopic methods. Simultaneous ^1H spectral information from other metabolites like Cho, Cr, Glu, Gly, and PE can be used to additionally characterize, classify, and distinguish healthy and tumor tissues. For both methods, ^{13}C and ^1H, diffusion weighting can be applied: multi-exponential diffusion attenuation can be used to distinguish intra- from extracellular signals due to a different diffusion characteristic (restricted and hindered diffusion). Based on a comparison with metabolites known to be intracellular as a reference, the intra/extracellular compartmentation of Lac in a tumor can be assessed. Finally, it is feasible to utilize not only steady-state information as performed in the current study, but also gain dynamic information from the labeling time course and ^{13}C turnover. In the case where ^{13}C label changes compartments, e.g., CSF, extracellular or intracellular space, this could possibly be detected dynamically by changes in the diffusion coefficients of metabolites during the time course of the study or in longer term.

To conclude, we have demonstrated the feasibility of diffusion $\{^1H–^{13}C\}$ spectroscopy in vivo, even at very large diffusion weighting of 50 ms/μm^2. To the best of our knowledge, we provided the first measurement of ADC values of ^{13}C Lac and ^{13}C Ala in the brain. This new technique was able to provide simultaneous information about metabolite diffusion and compartmentation in vivo. For intracerebral 9L glioma in the rat, we

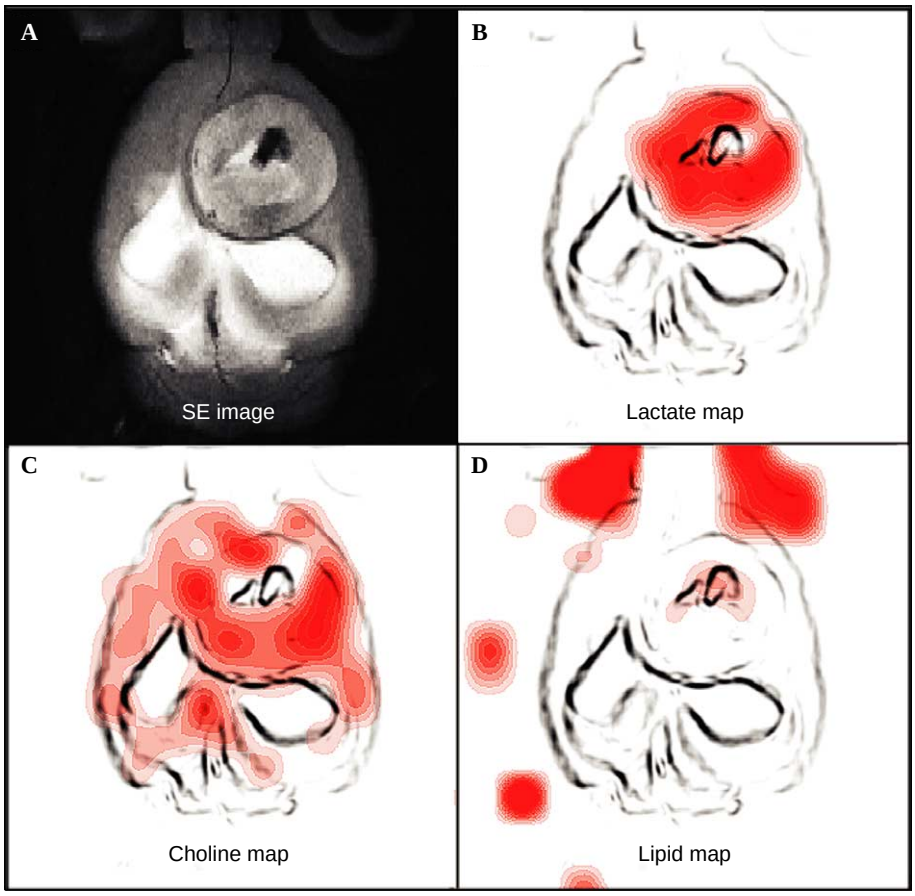

Fig. 6. Chemical shift images of Lac, Cho, and lipid in a 9L tumor in the rat brain compared to an axial T_2-weighted spin-echo image (A). Lac (B), Cho (C), and lipid CSI maps (D) are overlayed to an outline sketch of the anatomical image (A). Acquisition parameters: spin-echo sequence, FOV 2.5×2.5 cm^2, slice thickness 2 mm, TE 80 ms, TR 1.5 s, NA 1. CSI, *J*-difference edited, FOV 2.5×2.5 cm^2, slice thickness 2 mm, matrix size 16×16, TE 144 ms, TR 2.5 s, NA 4.

found that Lac is the major metabolic product of glycolysis and that at least some part of the metabolically active lactate is located in the intracellular space of tumor tissue. Spectroscopic maps of Lac and abnormally elevated Cho levels were consistently found only in tumor tissue and not in the surrounding and necrotic areas.

Acknowledgments

The authors thank Dr. Hellmut Merkle for expert technical assistance on the magnet systems. This work was supported by National Institutes of Health grants RR08079, CA64338, and the W.M. Keck Foundation.

References

[1] K. Nicolay, K.P. Braun, R.A. Graaf, R.M. Dijkhuizen, M.J. Kruiskamp, Diffusion NMR spectroscopy, NMR Biomed. 14 (2001) 94–111.
[2] R.A. Kauppinen, Monitoring cytotoxic tumour treatment response by diffusion magnetic resonance imaging and proton spectroscopy, NMR Biomed. 15 (2002) 6–17.
[3] R. Gruetter, S.A. Weisdorf, V. Rajanayagan, M. Terpstra, H. Merkle, C.L. Truwit, M. Garwood, S.L. Nyberg, K. Ugurbil, Resolution improvements in in vivo ^{1}H NMR spectra with increased magnetic field strength, J. Magn. Reson. 135 (1998) 260–264.
[4] J. Pfeuffer, I. Tkac, S.W. Provencher, R. Gruetter, Toward an in vivo neurochemical profile: quantification of 18 metabolites in short-echo-time ^{1}H NMR spectra of the rat brain, J. Magn. Reson. 141 (1999) 104–120.
[5] J. Pfeuffer, S.W. Provencher, R. Gruetter, Water diffusion in rat brain in vivo as detected at very large b values is multicompartmental, MAGMA 8 (1999) 98–108.
[6] J. Pfeuffer, I. Tkac, R. Gruetter, Extracellular-intracellular distribution of glucose and lactate in the rat brain assessed noninvasively by diffusion-weighted ^{1}H nuclear magnetic resonance spectroscopy in vivo, J. Cereb. Blood Flow Metab. 20 (2000) 736–746.
[7] P.C. van Zijl, C.T. Moonen, P. Faustino, J. Pekar, O. Kaplan, J.S. Cohen, Complete separation of intracellular and extracellular information in NMR spectra of perfused cells by diffusion-weighted spectroscopy, Proc. Natl. Acad. Sci. USA 88 (1991) 3228–3232.
[8] P.C. van Zijl, D. Davis, C.T. Moonen, Diffusion Spectroscopy in Living Systems, Academic Press, London, vol. 11, 1994, pp. 185–198.
[9] J. Pfeuffer, U. Flögel, W. Dreher, D. Leibfritz, Restricted diffusion and exchange of intracellular water: theoretical modelling and diffusion time dependence of ^{1}H NMR measurements on perfused glial cells, NMR Biomed. 11 (1998) 19–31.

[10] Y. Assaf, Y. Cohen, Non-mono-exponential attenuation of water and N-acetyl aspartate signals due to diffusion in brain tissue, J. Magn. Reson. 131 (1998) 69–85.
[11] Y. Mardor, O. Kaplan, M. Sterin, J. Ruiz-Cabello, E. Ash, Y. Roth, I. Ringel, J.S. Cohen, Noninvasive real-time monitoring of intracellular cancer cell metabolism and response to lonidamine treatment using diffusion weighted proton magnetic resonance spectroscopy, Cancer Res. 60 (2000) 5179–5186.
[12] T. Niendorf, R.M. Dijkhuizen, D.G. Norris, C. van Lookeren, K. Nicolay, Biexponential diffusion attenuation in various states of brain tissue: implications for diffusion-weighted imaging, Magn. Reson. Med. 36 (1996) 847–857.
[13] J. Karger, H. Pfeifer, W. Heink, Principles and application of self-diffusion measurements by nuclear magnetic resonance, Adv. Magn. Res. 12 (1988) 1–89.
[14] C. Nicholson, J.M. Phillips, Ion diffusion modified by tortuosity and volume fraction in the extracellular microenvironment of the rat cerebellum, J. Physiol. (Lond.) 321 (1981) 225–257.
[15] J. Pfeuffer, Beschränkte Diffusion und Austausch von Wasser in Zellkulturen und im Gehirn: Theoretische Modelle und 1H-NMR-Messungen [Restricted diffusion and exchange of water in cell cultures and in the brain: Theoretical models and 1H NMR measurements]. University of Bremen 1996, Dissertation, Universität Bremen 1996 Shaker Verlag, Aachen, 1997.
[16] M. Zhou, L. Frydman, Pulsed-gradient spin-echo measurements of anisotropic diffusion by dipole-decoupled ^{13}C nuclear magnetic resonance, Solid State Nucl. Magn. Reson. 4 (1995) 301–307.
[17] C. Malveau, B. Diter, F. Humbert, D. Canet, Self-diffusion measurements by carbon-13 NMR using radiofrequency field gradients, J. Magn. Reson. 130 (1998) 131–134.
[18] S.V. Dvinskikh, R. Sitnikov, I. Furo, 13C PGSE NMR experiment with heteronuclear dipolar decoupling to measure diffusion in liquid crystals and solids, J. Magn. Reson. 142 (2000) 102–110.
[19] J. Pfeuffer, I. Tkac, I.Y. Choi, H. Merkle, K. Ugurbil, M. Garwood, R. Gruetter, Localized in vivo ^{1}H NMR detection of neurotransmitter labeling in rat brain during infusion of [1-^{13}C] D-glucose, Magn. Reson. Med. 41 (1999) 1077–1083.
[20] R.A. Kauppinen, S.R. Williams, Cerebral energy metabolism and intracellular pH during severe hypoxia and recovery: a study using 1H, 31P, and 1H [13C] nuclear magnetic resonance spectroscopy in the guinea pig cerebral cortex in vitro, J. Neurosci. Res. 26 (1990) 356–369.
[21] J.C. Street, U. Mahmood, D. Ballon, A.A. Alfieri, J.A. Koutcher, 13C and 31P NMR investigation of effect of 6-aminonicotinamide on metabolism of RIF-1 tumor cells in vitro, J. Biol. Chem. 271 (1996) 4113–4119.
[22] A. Vivi, M. Tassini, H. Ben Horin, G. Navon, O. Kaplan, Comparison of action of the anti-neoplastic drug lonidamine on drug-sensitive and drug-resistant human breast cancer cells: 31P and 13C nuclear magnetic resonance studies, Breast Cancer Res. Treat. 43 (1997) 15–25.
[23] A.K. Bouzier, R. Goodwin, F.M. de Gannes, H. Valeins, P. Voisin, P. Canioni, M. Merle, Compartmentation of lactate and glucose metabolism in C6 glioma cells. A 13C and 1H NMR study, J. Biol. Chem. 273 (1998) 27162–27169.
[24] M. Terpstra, R. Gruetter, W.B. High, M. Mescher, L. DelaBarre, H. Merkle, M. Garwood, Lactate turnover in rat glioma measured by in vivo nuclear magnetic resonance spectroscopy, Cancer Res. 58 (1998) 5083–5088.
[25] M. Stubbs, P.M. McSheehy, J.R. Griffiths, C.L. Bashford, Causes and consequences of tumour acidity and implications for treatment, Mol. Med. Today 6 (2000) 15–19.
[26] A.K. Bouzier-Sore, P. Canioni, M. Merle, Effect of exogenous lactate on rat glioma metabolism, J. Neurosci. Res. 65 (2001) 543–548.
[27] J. Pfeuffer, J.C. Lin, K. Ugurbil, M. Garwood, Diffusion-weighted spectroscopy of ^{13}C-labeled lactate in rat glioma in vivo, in: Proceedings of the ISMRM, 8th Scientific Meeting, Denver, 2000, p. 475.
[28] J.C. Lin, L. DelaBarre, M. Garwood, A new method for editing lactate and detecting other ^{1}H metabolites simultaneously, in: Proceedings of the ISMRM, 8th Scientific Meeting, Denver, 2000, p. 375.
[29] I. Tkac, Z. Starcuk, I.Y. Choi, R. Gruetter, In vivo ^{1}H NMR spectroscopy of rat brain at 1 ms echo time, Magn. Reson. Med. 41 (1999) 649–656.
[30] R. Gruetter, I. Tkac, Field mapping without reference scan using asymmetric echo-planar techniques, Magn. Reson. Med. 43 (2000) 319–323.
[31] A. Tannus, M. Garwood, Improved Performance of Frequency-Swept pulses using offset-independent adiabaticity, J. Magn. Reson. A 120 (1996) 133–137.
[32] T.L. Hwang, P.C. van Zijl, M. Garwood, Asymmetric adiabatic pulses for NH selection, J. Magn. Reson. 138 (1999) 173–177.
[33] L.G. Longsworth, Diffusion measurements, at 25°, of aqueous solutions of amino acids, peptides, and sugars, J. Am. Chem. Soc. 75 (1953) 5705–5709.
[34] C.H. Sotak, A method for measuring the apparent self-diffusion coefficient of in-vivo lactic acid using double-quantum coherence transfer spectroscopy, J. Magn. Reson. 90 (1990) 198–204.
[35] D.M. Freeman, C.H. Sotak, H.H. Muller, S.W. Young, R.E. Hurd, A double quantum coherence transfer proton NMR spectroscopy technique for monitoring steady-state tumor lactic acid levels in vivo, Magn. Reson. Med. 14 (1990) 321–329.
[36] C.H. Sotak, Multiple quantum NMR spectroscopy methods for measuring the apparent self-diffusion coefficient of in vivo lactic acid, NMR Biomed. 4 (1991) 70–72.
[37] W.G. Kuhr, C.J. van den Berg, J. Korf, In vivo identification and quantitative evaluation of carrier-mediated transport of lactate at the cellular level in the striatum of conscious, freely moving rats, J. Cereb. Blood Flow Metab. 8 (1988) 848–856.
[38] W.G. Kuhr, J. Korf, Extracellular lactic acid as an indicator of brain metabolism: continuous on-line measurement in conscious, freely moving rats with intrastriatal dialysis, J. Cereb. Blood Flow Metab. 8 (1988) 130–137.
[39] M. Stubbs, P.M. McSheehy, J.R. Griffiths, Causes and consequences of acidic pH in tumors: a magnetic resonance study, Adv. Enzyme Regul. 39 (1999) 13–30.
[40] J.S. Cohen, M. Motiei, S. Carmi, D. Shiperto, O. Yefet, I. Ringel, Determination of intracellular pH and compartmentation using diffusion-weighted NMR spectroscopy with pH-sensitive indicators, Magn. Reson. Med. 51 (2004) 900–903.
[41] M.L. Garcia-Martin, G. Herigault, C. Remy, R. Farion, P. Ballesteros, J.A. Coles, S. Cerdan, A. Ziegler, Mapping extracellular pH in rat brain gliomas in vivo by ^{1}H magnetic resonance spectroscopic imaging: comparison with maps of metabolites, Cancer Res. 61 (2001) 6524–6531.